A Series-Resonance-Based Three-Port Converter with Unified Autonomous Control Method in DC Microgrids

Panbao Wang, Shuxin Zhang and Dianguo Xu
Department of Electrical Engineering
Harbin Institute of Technology
Harbin, 150001, China

Xiaonan Lu
Energy Systems Division
Argonne National Laboratory
Lemont, United States

***Abstract*—A three-port converter (TPC) as a compact DC/DC energy conversion unit can effectively integrate renewable energy sources (RESs) and energy storage systems (ESSs) into DC microgrids (MGs). In this paper, a hardware-decoupling approach using series-connected capacitor in a TPC is proposed and studied. In this series-resonance-based TPC, the decoupled power flow model among different ports is derived based on the equivalent model of the converter and the operation principle of the resonant circuit. Considering the characteristics and operation modes of photovoltaic (PV) and energy storage unit (ESU), which are connected at the two input ports of the TPC, a unified control method based on minimum value competition logic is proposed to achieve voltage regulation of the common bus in DC MGs. Experimental results are obtained in different test scenarios to demonstrate the effectiveness of the proposed method.**

Keywords—three-port converter; series resonance; autonomous control; dc microgrids

I. INTRODUCTION

The topologies and operation principles of both isolated and non-isolated three-port converters (TPCs) have been extensively studied in the past years [1]-[5]. Since only a single energy conversion stage is needed, a TPC features the advantages of high power density and high energy conversion efficiency [6]. Compared to independent DC/DC converters, these advantages of TPC make it a suitable candidate for effectively integrating photovoltaics (PVs) and energy storage units (ESUs), and thereby integrating them into microgrids (MGs) [7]. A non-isolated buck/boost-converter-based three-port converter (TPC) is proposed in [8]. Meanwhile, many different kinds of isolated TPC topologies have been developed [9], [10]. Compared to traditional buck/boost converters, isolated multi-port converters feature the characteristics of high voltage conversion ratio, electrical isolation etc. In addition, by using phase-shifting control [11], the soft switching control in the multi-port converter with a full-bridge configuration is easy to be achieved [12].

Since the converter circuits and the flux of transformer are commonly shared in a TPC, the power flow among different ports are usually coupled. Therefore, it is necessary to study the decoupling method so that dynamic response and independent control of power flow among different ports can be improved [13]. In [14], the topology with triple active bridges and a three-winding high-frequency transformer is adopted to constitute a full isolated TPC. The power flow in the TPC is analyzed, and a decoupling matrix is added in the proposed power decoupling control diagram. In [15], a comprehensive control method with phase-shifting and plus duty cycle regulation is applied in a half-bridge-based isolated TPC. In addition, based on full isolated TPC, resonant capacitors are used to construct two series-resonance networks in the TPC [16]. Thus sinusoidal currents can be obtained at the high-frequency transformer winding side.

In this paper, by inserting a capacitor in series with the bridge inductor at one port, the hardware decoupling characteristic of series-resonance-based TPC is implemented and analyzed, and the TPC is employed to integrate PV and ESU, which are further connected to DC MGs. Hardware decoupling method can improve the response of the TPC and simplify the control system. Besides, since sinusoidal currents is achieved, the operation temperature of the transformer can be greatly reduced. Additionally, a unified control method based on minimum value competition logic is proposed to realize autonomous control between PV and ESU in DC MGs. Simulation and experimental results in different test scenarios demonstrate the effectiveness of the proposed method.

II. SERIES RESONANCE BASED TPC

As shown in Fig. 1 (a), port #1, #2, #3 of the TPC are connected to PV, ESU and common DC bus of DC MG, respectively. As an example circuit, two full bridges are used in port #1 and port #3 of the TPC, and port 2# is interfaced with an active half bridge unit, where a resonant capacitor is connected in series at the bridge arm. This series resonant network is used to reduce the power coupling effects among the converter ports, i.e., to realize hardware decoupling. The power exchange between any two ports of the TPC can be controlled by adjusting the corresponding phase-shifting angle.

The work conducted by P. Wang, S. Zhang and D. Xu was supported by the National Natural Science Foundation of China (51707045).

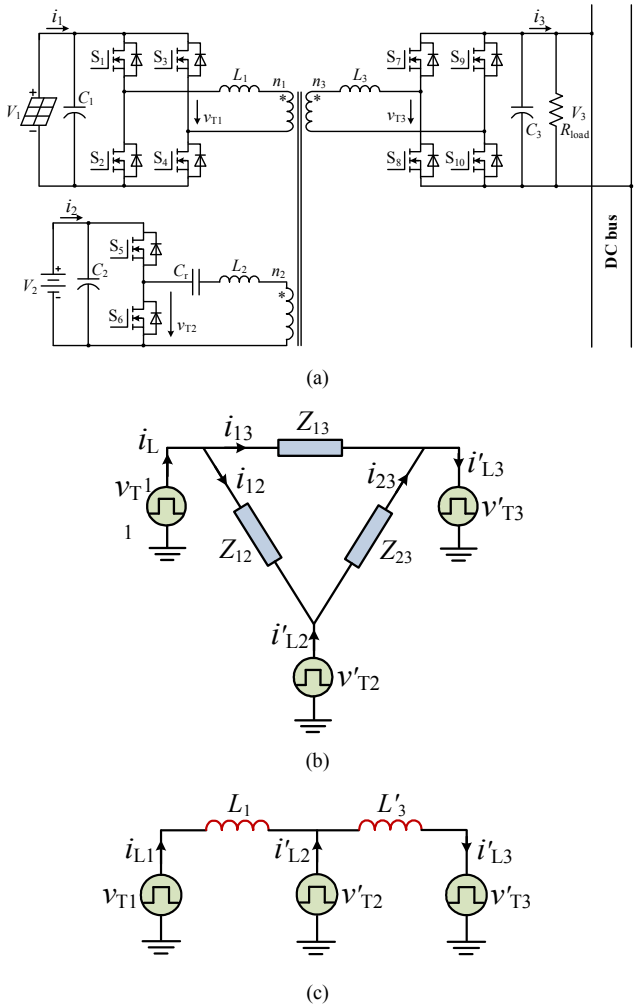

Fig. 1. Series-resonance-based TPC: (a) Circuit topology, (b) Δ-type equivalent circuit model, (c) Equivalent circuit model when L_{2eq} is approximately equal to zero by inserting the resonant capacitor.

The principle of hardware decoupling is presented as follows. With the inserted resonant capacitor, the equivalent bridge inductance L_{2eq} can be expressed as:

$$\omega_r L_{2eq} = X_2 = \omega_r L_2 - \frac{1}{\omega_r C_r} = \omega_r L_2 - \omega_r L_r = \omega_r (L_2 - L_r) \quad (1)$$

where ω_r is the angular resonant frequency, and L_r is the series resonant equivalent inductance.

It is indicated in (1) that the bridge inductor at port #2 becomes smaller or even reduces to zero after deploying the resonant capacitor.

Furthermore, by merging L_{2eq} into the winding of port #1, the Δ-type branch impedance of the TPC, as shown in Fig. 1 (b), can be obtained:

$$\begin{cases} Z_{12} = j\omega_r L_{12} = j\omega_r L_1 + j\omega_r L'_{2eq} + j\omega_r \dfrac{L_1 \cdot L'_{2eq}}{L'_3} \\ Z_{23} = j\omega_r L_{23} = j\omega_r L'_{2eq} + j\omega_r L'_3 + j\omega_r \dfrac{L'_{2eq} \cdot L'_3}{L_1} \\ Z_{13} = j\omega_r L_{13} = j\omega_r L_1 + j\omega_r L'_3 + j\omega_r \dfrac{L_1 \cdot L'_3}{L'_{2eq}} \end{cases} \quad (2)$$

where L'_{2eq} and L'_3 are the equivalent bridge inductors of the Δ-type equivalent circuit model at port #2 and port #3 , respectively.

Hence, the power flow between neighboring ports can be thereby derived and expressed as:

$$\begin{cases} p_1 = p_{12} = \dfrac{V_1 V'_2}{2|Z_{12}|}\varphi_{12}\left(1-\dfrac{|\varphi_{12}|}{\pi}\right) = \dfrac{V_1 V'_2}{2\omega_r L_1}\varphi_{12}\left(1-\dfrac{|\varphi_{12}|}{\pi}\right) \\ p_2 = p_{23} - p_{12} = \dfrac{V'_2 V'_3}{2|Z_{23}|}\varphi_{23}\left(1-\dfrac{|\varphi_{23}|}{\pi}\right) - \dfrac{V_1 V'_2}{2|Z_{12}|}\varphi_{12}\left(1-\dfrac{|\varphi_{12}|}{\pi}\right) \\ \quad = \dfrac{V'_2 V'_3}{2\omega_r L'_3}\varphi_{23}\left(1-\dfrac{|\varphi_{23}|}{\pi}\right) - \dfrac{V_1 V'_2}{2\omega_r L_1}\varphi_{12}\left(1-\dfrac{|\varphi_{12}|}{\pi}\right) \\ p_3 = p_{23} = \dfrac{V'_3}{2|Z_{23}|}\varphi_{23}\left(1-\dfrac{|\varphi_{23}|}{\pi}\right) = \dfrac{V'_2 V'_3}{2\omega_r L'_3}\varphi_{23}\left(1-\dfrac{|\varphi_{23}|}{\pi}\right) \end{cases} \quad (3)$$

where φ_{12} is the phase-shifting value between port #1 and port #2, and φ_{23} is the phase-shifting value between port #2 and port #3.

Therefore, when L_{2eq} is approximately equal to zero, the equivalent impedance Z_{13} between port #1 and port #3 increases. Meanwhile, Z_{12} and Z_{23} decrease and gradually become $\omega_r L_1$ and $\omega_r L'_3$, which forces the power exchange between port #1 and port #3 to lower down significantly. By selecting a suitable resonance capacitor, the equivalent circuit with hardware decoupling can be derived and shown in Fig. 1 (c). Consequently, the series resonant network can reduce the coupling effects among three ports of TPC.

III. Proposed Control Method

In this PV-ESU TPC system, the control objectives include input power control at PV port, voltage-limiting/power-limiting control and charging/discharging control at ESU port and constant voltage control at DC bus port. Since only N-1 control variables can be adjusted in a N-port converter, two phase-shifting control variables i.e. φ_{12} and φ_{23} are selected in this paper. In order to maximize the utilization of the PV power and provide continuous and reliable power to local loads in islanded control mode, the PV unit should be operated in maximum power point tracking (MPPT) mode, and ESU should balance the long-term power in DC MG and respond to the power fluctuations induced by PV or loads.

After analyzing the control objectives and the hardware decoupling of the series-resonance-based TPC, a unified

control method is proposed to realize autonomous control of PV and ESU in DC MGs. As shown in Fig. 2, the proposed control scheme is comprised of PV power regulator (PVPR), battery voltage/current regulator (BVR/BCR), DC voltage regulator (DCVR) and competition logic module. Compared to conventional independent control strategies of PV, battery and output DC bus voltage, the unified control scheme can ensure a smooth transition between different operation modes.

The minimum value competition logic is detailed in Fig. 2 as highlighted in orange. Particularly, in the constant voltage operation mode of DC MG, the DCVR always regulates phase-shifting angle φ_{23} to maintain constant output voltage at the DC output side. When the state-of-charge (SoC) of the battery does not violate its upper limit, φ_{12} is adjusted by PVPR to achieve MPPT. Meanwhile, the battery is used to automatically compensate the power mismatch. When the SoC of the battery reaches its limits or its charging current violates its upper threshold, φ_{12} is controlled by BVR or BCR instead of PVPR. In this operation condition, the MPPT of PV source is terminated accordingly. Therefore, by using a minimum value competition logic, the outputs of PVPR, BVR and BCR can regulate φ_{12} autonomously.

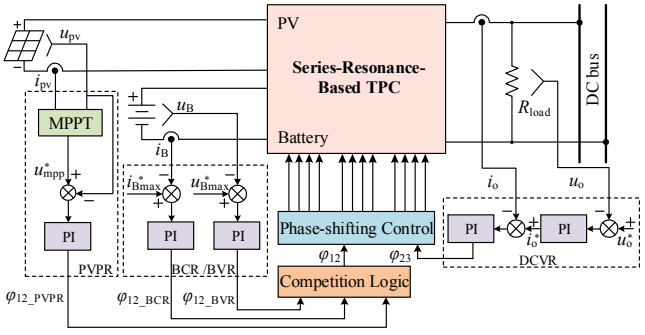

(a)

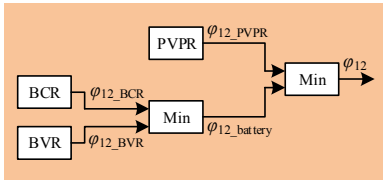

(b)

Fig. 2. Proposed control scheme for the TPC.

IV. Experimental Results

The effectiveness of the proposed unified autonomous control is verified in simulation environment in different test scenarios.

As shown in Fig. 3, when the maximum power point (MPP) of the PV panel changes from 485 W to 480 W at 0.1 s, the TPC can track the new MPP in a fast response and the voltage at the load side (i.e., port #3) keeps constant. The achieved power balance by ESU can also be observed in this period at port #2.

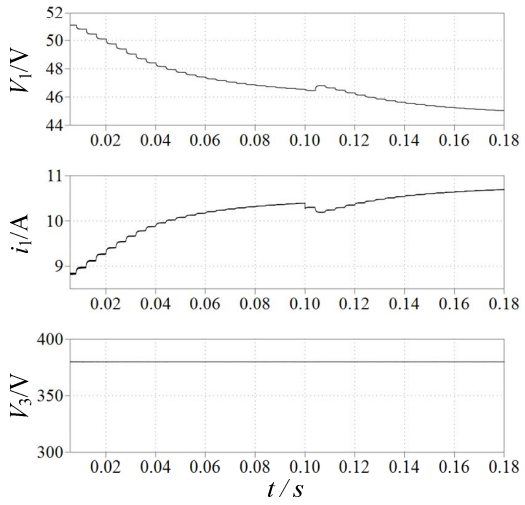

(a)

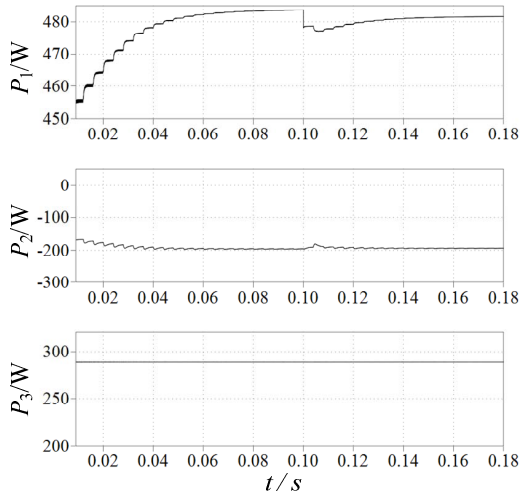

(b)

Fig. 3. Simulation results for MPPT: (a) Voltage and current of port #1 and #3, (b) Power of each port.

The simulation results for ESU reaching charging limit are shown in Fig. 4. The upper voltage limit of the charging process is set at 110 V and competition logic values of phase-shifting angle in the proposed unified autonomous control are also be recorded. As seen in Fig. 4, when the voltage of ESU reaches 110 V, BVR exits the saturation state. When $\varphi_{12\_BVR} < \varphi_{12\_PVPR}$, BVR wins in the logic of competition and starts dominating the regulation of φ_{12}.

Accordingly, the ESU port stops charging and maintains zero power exchange. The power exchange at the PV port decreases to meet the power balance sources and loads. It can be also observed that during the adjusting process, the phase-shifting angle and the power exchange at each port have no overshoot, and the voltage at the load port is not affected by the change of the system operate mode.

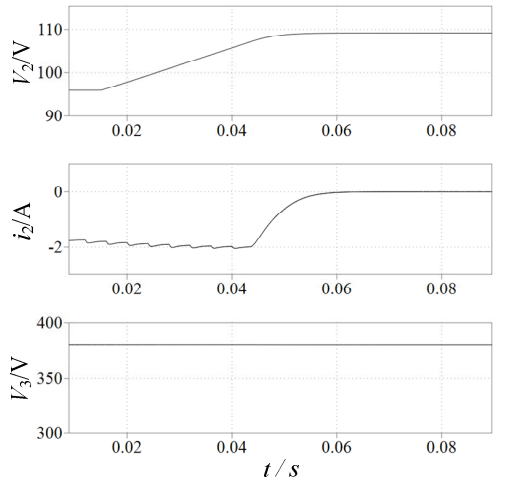

(a)

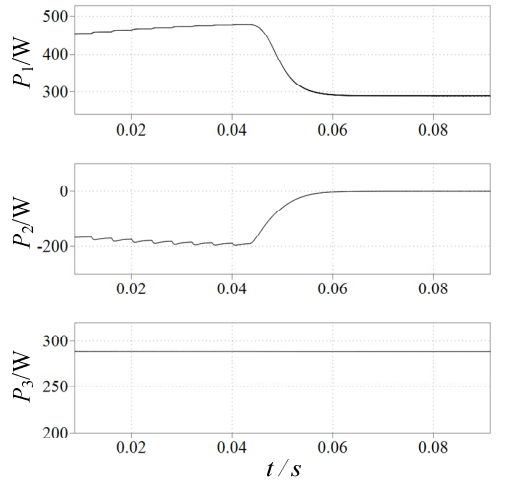

(b)

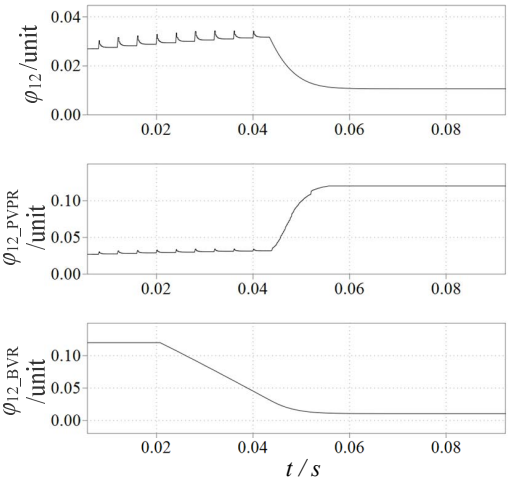

(c)

Fig. 4. Simulation results for ESU reaching charging limit: (a) Voltage and current of ESU and load voltage, (b) Power of each port, (c) Values of phase-shifting angle.

Further, two experimental scenarios are designed and tested using the TPC prototype.

First, by reducing the maximum output power of PV simulator at $t = t_1$, as seen in Fig. 5 (a), the output power of port #1 is reduced accordingly, and the power exchange at port #3 keeps constant. In Fig. 5 (b), also at $t = t_1$, the voltage of port #1 starts increasing, which means the MPPT algorithm tracks the new operating point. Meanwhile, the current at port #2 increases, indicating that insufficient power is supplied by the PV and the battery is controlled to automatically compensate the power mismatch. In addition, the DC bus voltage keeps constant in the whole process.

If the battery reaches its charging limit, rather than being controlled by the PVPR module, the phase shifting angle φ_{12} is regulated by the BVR module instead, and the PV exits MPPT mode. As shown in Fig. 6 (a) and (b), in this scenario, the charging current of battery becomes zero and the output power of PV decreases accordingly to maintain power balance.

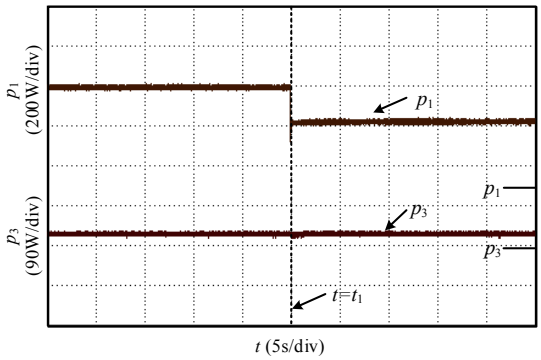

(a)

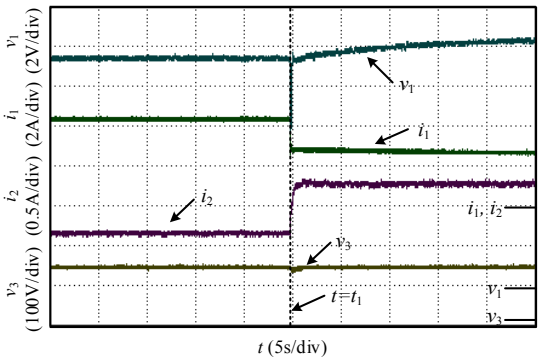

(b)

Fig. 5. Experimental results for PV power reducing: (a) Powers of port #1 and #3, (b) Voltages and currents of port #1, #2 and #3.

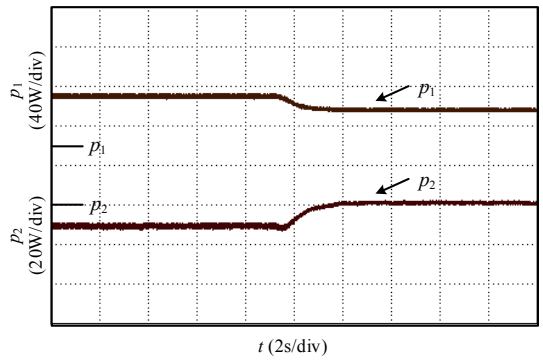

(a)

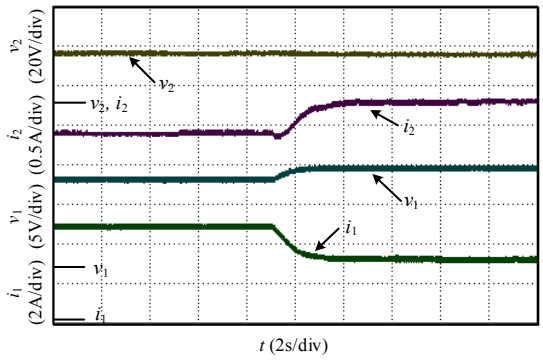

(b)

Fig. 6. Experimental results for ESU reaching charging limit: (a) Powers of port #1 and #2, (b) Voltages and currents of port #1 and #3.

V. CONCLUTION

The series-resonance-based TPC is implemented as an interface converter for integrating PV, ESU into DC MGs. The series-resonant network in the TPC can reduce the coupling effects among different ports, and a unified control method based upon competition logic module is thereby proposed. Detailed simulation and experimental results verify the effectiveness of the proposed control method in the illustrative test scenarios of PV power curtailment and battery charging saturation. Simulation and experimental results indicate that based on the hardware decoupling method and unified autonomous control method, two phase-shifting angles can be by controlled sequentially by using thecompetition logic module in different operate modes, and power decoupling effect and autonomous control can be realized effectively.

REFERENCES

[1] P. Zhang, Y. Chen and Y. Kang, "Nonisolated Wide Operation Range Three-Port Converters With Variable Structures," IEEE Journal of Emerging and Selected Topics in Power Electronics, vol. 5, no. 2, pp. 854-869, June 2017.

[2] H. Wu, K. Sun, R. Chen, H. Hu and Y. Xing, "Full-Bridge Three-Port Converters With Wide Input Voltage Range for Renewable Power Systems," IEEE Transactions on Power Electronics, vol. 27, no. 9, pp. 3965-3974, Sept. 2012.

[3] M. C. Mira, Z. Zhang, A. Knott and M. A. E. Andersen, "Analysis, Design, Modeling, and Control of an Interleaved-Boost Full-Bridge Three-Port Converter for Hybrid Renewable Energy Systems," IEEE Transactions on Power Electronics, vol. 32, no. 2, pp. 1138-1155, Feb. 2017.

[4] J. Zhang, H. Wu, Y. Xing, H. Hu and F. Cao, "Power management of a modular three-port converter-based spacecraft power system," IEEE Transactions on Aerospace and Electronic Systems, vol. 52, no. 1, pp. 486-492, February 2016.

[5] H. Zhu, D. Zhang, Q. Liu and Z. Zhou, "Three-Port DC/DC Converter With All Ports Current Ripple Cancellation Using Integrated Magnetic Technique," IEEE Transactions on Power Electronics, vol. 31, no. 3, pp. 2174-2186, March 2016.

[6] K. Itoh, M. Ishigaki, N. Yanagizawa, S. Tomura and T. Umeno, "Analysis and Design of a Multiport Converter Using a Magnetic Coupling Inductor Technique," IEEE Transactions on Industry Applications, vol. 51, no. 2, pp. 1713-1721, March-April 2015.

[7] P. Wang, X. Lu, X. Yang, W. Wang and D. Xu, "An Improved Distributed Secondary Control Method for DC Microgrids With Enhanced Dynamic Current Sharing Performance," IEEE Transactions on Power Electronics, vol. 31, no. 9, pp. 6658-6673, Sept. 2016.

[8] H. Wu, J. Zhang and Y. Xing, "A Family of Multiport Buck–Boost Converters Based on DC-Link-Inductors (DLIs)," IEEE Transactions on Power Electronics, vol. 30, no. 2, pp. 735-746, Feb. 2015.

[9] Haimin Tao, J. L. Duarte and M. A. M. Hendrix, "Multiport converters for hybrid power sources," IEEE Power Electronics Specialists Conference, Rhodes, 2008, pp. 3412-3418

[10] H. Zhu, D. Zhang, H. S. Athab, B. Wu and Y. Gu, "PV Isolated Three-Port Converter and Energy-Balancing Control Method for PV-Battery Power Supply Applications," IEEE Transactions on Industrial Electronics, vol. 62, no. 6, pp. 3595-3606, June 2015.

[11] S. Inoue and H. Akagi, "A Bidirectional DC–DC Converter for an Energy Storage System With Galvanic Isolation," IEEE Transactions on Power Electronics, vol. 22, no. 6, pp. 2299-2306, Nov. 2007.

[12] Z. Wang and H. Li, "An Integrated Three-Port Bidirectional DC–DC Converter for PV Application on a DC Distribution System," IEEE Transactions on Power Electronics, vol. 28, no. 10, pp. 4612-4624, Oct. 2013.

[13] W. Wang, P. Wang, T. Ma, H. Liu and H. Wu, "A simple decoupling control method for isolated three-port bidirectional converter in low-voltage DC microgrids," 2015 IEEE Energy Conversion Congress and Exposition (ECCE), Montreal, QC, 2015, pp. 3192-3196.

[14] C. Zhao, S. D. Round and J. W. Kolar, "An Isolated Three-Port Bidirectional DC-DC Converter With Decoupled Power Flow Management," IEEE Transactions on Power Electronics, vol. 23, no. 5, pp. 2443-2453, Sept. 2008.

[15] L. Wang, Z. Wang and H. Li, "Asymmetrical Duty Cycle Control and Decoupled Power Flow Design of a Three-port Bidirectional DC-DC Converter for Fuel Cell Vehicle Application," IEEE Transactions on Power Electronics, vol. 27, no. 2, pp. 891-904, Feb. 2012.

[16] H. Krishnaswami and N. Mohan, "Three-Port Series-Resonant DC–DC Converter to Interface Renewable Energy Sources With Bidirectional Load and Energy Storage Ports," IEEE Transactions on Power Electronics, vol. 24, no. 10, pp. 2289-2297, Oct. 2009.